Rare Metal Materials and Engineering
Volume 50, Issue 9, September 2021
Available online at www.rmme.ac.cn

Science Press

Cite this article as: Zhang Xiaoxue, Du Jiangfei, Peng Feifei, et al. Phase Transformations and Thermodynamics Analysis of Hydrogen Absorption of Ti6Al4V Alloy[J]. Rare Metal Materials and Engineering, 2021, 50(09): 3043-3049.

ARTICLE

Phase Transformations and Thermodynamics Analysis of Hydrogen Absorption of Ti6Al4V Alloy

Zhang Xiaoxue[1], Du Jiangfei[2], Peng Feifei[3], Xiao Xingmao[3], Yuan Baoguo[2]

[1] Anhui Sanlian University, Hefei 230601, China; [2] Hefei University of Technology, Hefei 230009, China; [3] Southwest Technology and Engineering Research Institute, Chongqing 400039, China

Abstract: Thermodynamics of hydrogen absorption and phase transformations in Ti6Al4V alloy were investigated by pressure-composition (*P*-*C*) isotherm measurement at hydrogenation temperatures in the range of 823~1023 K. Results show that the hydrogen pressure is increased with increasing the hydrogen content when Ti6Al4V alloy is hydrogenated at different temperatures. Only one sloped pressure plateau occurs in each *P*-*C* isotherm during the hydrogenation treatment because of the existence of original β phase in Ti6Al4V alloy. According to Vant's Hoff law, the values of enthalpy and entropy of the pressure plateau region are -50.7±0.26 kJ/mol and -138.4±0.69 $J \cdot K^{-1} \cdot mol^{-1}$, respectively. The Sieverts constant increases firstly and then decreases gradually with increasing the hydrogenation temperature. The phase composition and phase transformation of Ti6Al4V alloy during the hydrogenation treatment were analyzed.

Key words: titanium alloy; hydrogen absorption; thermodynamics; phase transformation

Recently, thermo-hydrogen processing (THP) has been widely investigated and applied to titanium and related alloys. THP is a technique using hydrogen as a temporary alloying element in titanium alloys to modify the microstructures and improve the mechanical properties of titanium alloys[1-5]. THP can improve the room-temperature plasticity[6-8], decrease the flow stress in hot forging[9-11], and enhance the superplastic forming behavior[12-14] of titanium alloys. Yuan et al[6,8] investigated the room-temperature compressive properties of titanium alloys and found that hydrogen can improve the room-temperature plasticity of Ti6Al4V and TC21 alloys. THP is regarded as a gas-solid reaction, and its thermodynamics and parameters of hydrogenation reaction need to be studied further to optimize the hydrogenation reaction. The thermodynamic parameters of hydrogenation reaction can be determined through the relationship among hydrogen pressure (*P*), hydrogenation temperature (*T*), and hydrogen content (*C*). Shen et al[15] measured the hydrogenation *P*-*C* isotherms of pure titanium and Ti6Al4V alloy at 823~973 K and calculated the thermodynamic parameters of hydrogenation reaction. Wang et al[16] measured the hydrogenation *P*-*C*-*T* curves of TC21 alloy at 898~973 K and calculated thermodynamic parameters of hydrogenation reaction. However, the microstructure evolutions of titanium alloy after measurement of *P*-C isotherms at different hydrogenation temperatures were seldom studied.

In this research, *P*-*C* isotherms of Ti6Al4V alloy hydrogenated at 823~1023 K were investigated. Thermodynamic parameters of hydrogenation reaction were calculated. Microstructure evolutions of Ti6Al4V alloy after measurement of *P*-*C* isotherms at different hydrogenation temperatures were analyzed. The effects of hydrogenation temperature on phase composition and phase transformation of Ti6Al4V alloy were discussed.

1 Experiment

The material was Ti6Al4V alloy bars with a diameter of 6 mm and a height of 9 mm. Thermodynamic experiments of hydrogen absorption of Ti6Al4V alloy were conducted using continuously multistep method in a tube-type furnace.

Received date: February 04, 2021
Foundation item: National Natural Science Foundation of China (51875157); University Natural Science Research Project of Anhui Province (KJ2019A0894); Key Program of Natural Science of Anhui Sanlian University (KJZD2019005)
Corresponding author: Yuan Baoguo, Ph. D., Professor, School of Materials Science and Engineering, Hefei University of Technology, Hefei 230009, P. R. China, E-mail: yuanbaoguo@163.com

Ti6Al4V alloy specimens were hydrogenated in hydrogen atmosphere at different hydrogenation temperatures of 823~1023 K with an interval of 50 K. The initial hydrogen pressure was 20.325 kPa lasting for 1 h, and then hydrogen of 8 kPa was inflated with an interval of an hour. When the difference between the initial hydrogen pressure and the hydrogen pressure after heat preservation for 1 h during the hydrogenation treatment was lower than 0.5 kPa, the hydrogenation treatment was finished. Finally, the Ti6Al4V alloy specimens were air-cooled to room temperature. The actual hydrogen content was determined by weighing the specimen before and after hydrogenation treatment using an electronic analytical balance (SHIMADZU AUW220D). Hydrogen content in the hydrogenated Ti6Al4V alloy specimens was expressed as H/M (ratio of hydrogen to metal atoms).

Microstructures were observed by an optical microscope (OM, Carl Zeiss Lab. A1). A mixed solution (1 mL hydrofluoric acid, 1 mL nitric acid, and 8 mL water) was used to etch the OM specimens. Phase analysis was identified by X-ray diffraction (XRD, X'Pert PRO MPD) with Cu Kα radiation under 40 kV and 40 mA and a scanning rate of 3°/min. Foils for transmission electron microscopy (TEM, TECNAI G2 F20) analysis were mechanically thinned to about 120 μm and then milled by an ion milling equipment (MODEL-691) with voltage of 5 kV and incidence angle of 4°.

2 Results and Discussion

2.1 *P-C* isotherms

The *P-C* isotherms of Ti6Al4V alloys hydrogenated at different temperatures are shown in Fig.1. Hydrogen pressure is increased with increasing the hydrogen content when Ti6Al4V alloy is hydrogenated at different temperatures. The *P-C* isotherms of Ti6Al4V alloys hydrogenated at temperatures of 823~973 K are divided into three repions, which agrees with the results in Ref.[16]. The solubility of hydrogen in α phase and β phase gradually reaches saturation with increasing the hydrogen content after hydrogen atoms reach the surface of Ti6Al4V alloy, i. e., the first region. With increasing the hydrogen content, the phase transformation from α_H into β_H and hydride occur with a sloped pressure plateau, which is the second region. There is only one pressure plateau during the hydrogenation treatment for each *P-C* isotherm of Ti6Al4V alloys hydrogenated at temperatures of 823~973 K, because of the existence of original β phase in Ti6Al4V alloy[15]. The pressure plateau becomes more sloped and the length of the second region becomes shorter with increasing the hydrogenation temperature. The pressure plateau is not obvious when Ti6Al4V alloy was hydrogenated at 1023 K, indicating that the phase transformation from α_H into β_H is finished quickly and the *P-C* isotherm enters into the third region[16]. The reaction of titanium and hydrogen atoms to generate hydride ($Ti+xH \rightleftharpoons TiH_x$) is an exothermic reaction ($\Delta H<0$)[17]. Therefore, the formation of hydride is hindered at high hydrogenation temperature. The third region is dominated by the solubility of hydrogen in β_H phase and hydride. When hydrogen pressure reaches the similar status, the hydrogen content increases firstly and then decreases with increasing the hydrogenation temperature during the hydrogenation treatment of Ti6Al4V alloy. When hydrogen content reaches the similar value, the hydrogen pressure decreases firstly and then increases with increasing the hydrogenation temperature during the hydrogenation treatment of Ti6Al4V alloy.

2.2 Thermodynamic parameters

The enthalpy and entropy of the pressure plateau region during the hydrogenation treatment of Ti6Al4V alloy are calculated by Vant's Hoff law, as expressed by Eq.(1)[15,16].

$$\ln P_{H_2} = \frac{\Delta H}{RT} - \frac{\Delta S}{R} \quad (1)$$

where P_{H_2} is the equilibrium hydrogen pressure; T is the hydrogenation temperature; R is the ideal gas constant; ΔH is the enthalpy of formation; ΔS is the entropy of formation. The relationship between hydrogen pressure and hydrogenation temperature is shown in Fig.2, and the corresponding enthalpy and entropy of the pressure plateau region in Ti6Al4V alloy are listed in Table 1. Error exists because of the sloped pressure plateau after analysis of the results of enthalpy and entropy. Therefore, the average values of hydrogen pressure in the pressure plateau region during the hydrogenation treatment

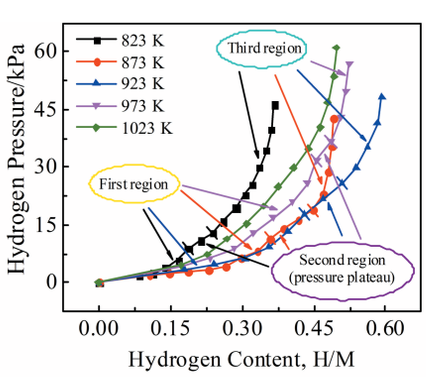

Fig.1 *P-C* isotherms of Ti6Al4V alloys hydrogenated at different temperatures

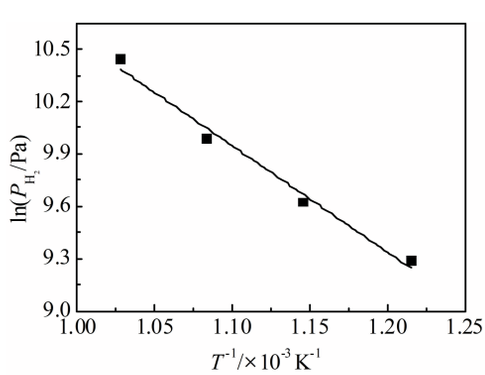

Fig.2 Relationship of hydrogen pressure-hydrogenation temperature of Ti6Al4V alloy

Table 1 Enthalpy and entropy of pressure plateau region of Ti6Al4V alloy

Temperature/K	Plateau pressure/Pa	ΔH/kJ·mol^{-1}	ΔS/J·K^{-1}·mol^{-1}
823	10 825	−50.7±0.26	−138.4±0.69
873	15 137.5		
923	21 825		
973	34 325		

Table 2 Sieverts constant K_S of Ti6Al4V alloys hydrogenated at different temperatures

Temperature/K	K_S
823	0.446
873	0.697
923	0.723
973	0.584
1023	0.560

of Ti6Al4V alloy are used to calculate the values of enthalpy and entropy for reducing the error. The average values of enthalpy and entropy of the pressure plateau region are −50.7±0.26 kJ/mol and −138.4±0.69 J/K·mol, respectively.

According to the Sieverts law, the relationship between hydrogen pressure P_{H_2} and hydrogen content C (H/M) can be expressed by Eq.(2)[18] as follows:

$$K_S = \frac{C}{(P_{H_2})^{1/2}} \quad (2)$$

where K_S is the corresponding Sieverts constant. The relationship between H/M and $(P_{H_2})^{1/2}$ during the hydrogenation treatment of Ti6Al4V alloy is presented in Fig. 3. Values of K_S for Ti6Al4V alloys hydrogenated at different temperatures were obtained by Eq. (2) and are listed in Table 2. From Table 2, it can be seen that the Sieverts constant increases firstly and then decreases gradually with increasing the hydrogenation temperature. The chemical activity and diffusion coefficient of titanium alloys are lower when the hydrogenation temperature is 823 K. The increase of Sieverts constant with increasing the hydrogenation temperature is caused by the increase of chemical activity and diffusion coefficient of the alloys. The Sieverts constant reaches its maximum value when the hydrogenation temperature is 923 K, indicating that the titanium atoms have the maximal affinity with hydrogen atoms at 923 K. When the hydrogenation temperature exceeds 923 K, the Sieverts constant is decreased with increasing the hydrogenation temperature, because the hydride becomes unstable and even decomposes at higher temperatures, and the solubility of hydrogen in the alloys is decreased with increasing the hydrogenation temperature.

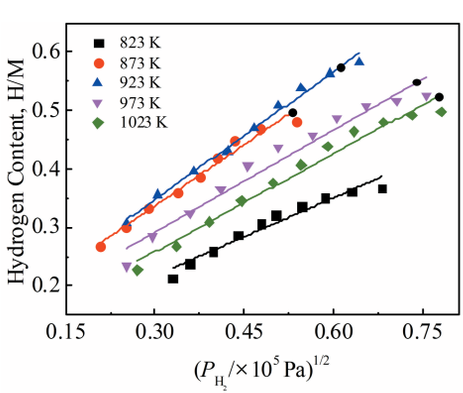

Fig.3 Relationship between H/M and $(P_{H_2})^{1/2}$ during the hydrogenation treatment of Ti6Al4V alloy

2.3 Microstructure evolution

2.3.1 OM observation

OM images of the as-received Ti6Al4V alloy and alloys hydrogenated at different temperatures are shown in Fig. 4. The lamellar microstructure of the as-received Ti6Al4V alloy is shown in Fig. 4a, in which α phase is light and β phase is dark. Microstructures of Ti6Al4V alloys after measurement of P-C isotherms at different hydrogenation temperatures change obviously. As shown in Fig. 4b and 4c, the microstructure is still lamellar when Ti6Al4V alloy is hydrogenated at 823 and 923 K, but the content of α phase and β phase changes reversely, compared with that in as-received Ti6Al4V alloy. This is because the addition of hydrogen in Ti6Al4V alloy changes the relative chemical potential of α phase and β phase[19,20]. The chemical potential of α phase becomes weak because of the precipitation of hydride in α phase, which causes the elastic or plastic strains, internal stresses, dislocation, and crystal defects[20]. In addition, cracks can be found in Ti6Al4V alloy hydrogenated at 823 K (Fig.4b), indicating that many hydrides are precipitated. After Ti6Al4V alloy is hydrogenated at 1023 K, the lamellar microstructure cannot be observed, but tiny acicular α' martensite and wide acicular α" martensite can be found in the alloy, as shown in Fig.4d.

2.3.2 XRD analysis

XRD patterns of the as-received Ti6Al4V alloy and alloys hydrogenated at different temperatures are shown in Fig. 5. As shown in Fig. 5a, the as-received Ti6Al4V alloy contains a large amount of α phase and a small amount of β phase. XRD patterns of Ti6Al4V alloy change obviously after hydrogenation at different temperatures. The relative intensities of diffraction peaks of β phase are increased with increasing the hydrogenation temperature, as shown in Fig. 5b~5d, suggesting that the amount of β phase is increased with increasing the hydrogenation temperature. The diffraction peaks of δ hydride appear in the XRD patterns of hydrogenated Ti6Al4V alloys. XRD patterns of Ti6Al4V alloys hydrogenated at 823 and 923 K are similar, but show significant difference from the case at 1023 K. Some diffraction peaks of α_2 phase (Ti_3Al) with hexagonal close packed (hcp) structure can be observed when the hydrogenation temperatures are 823 and 923 K, as shown in Fig. 5b and 5c. When the hydrogenation temperature is 1023 K, the diffraction peaks of α_2 phase disappear, and the diffraction peaks of hcp α' martensite and orthorhombic α"

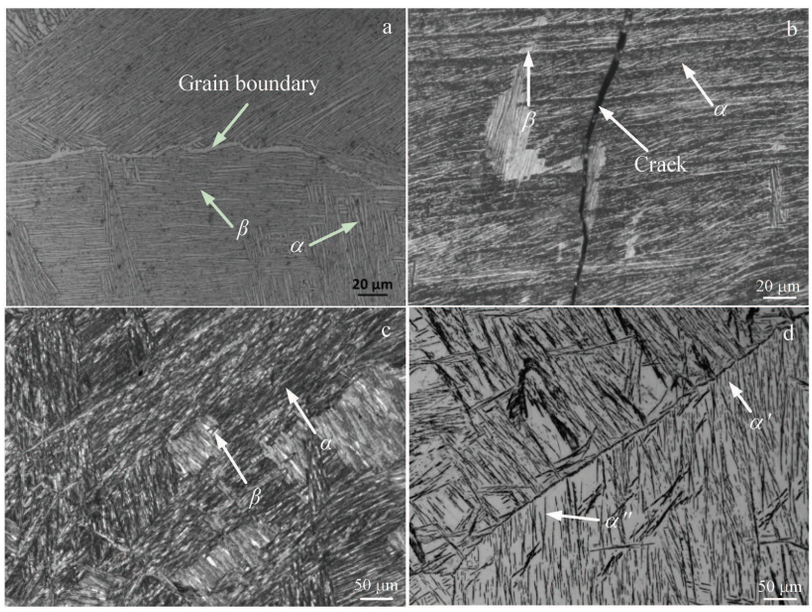

Fig.4 OM images of Ti6Al4V alloys before (a) and after hydrogenation at 823 K (b), 923 K (c), and 1023 K (d)

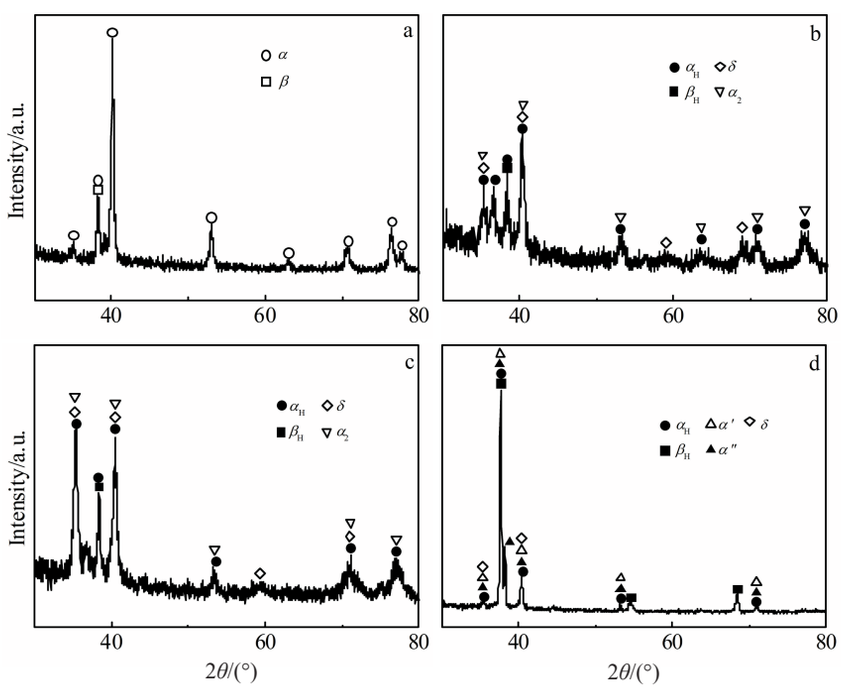

Fig.5 XRD patterns of Ti6Al4V alloys before (a) and after hydrogenation at 823 K (b), 923 K (c), and 1023 K (d)

martensite appear, as shown in Fig.5d.

2.3.3 TEM analysis

TEM images of Ti6Al4V alloys hydrogenated at different temperatures are shown in Fig. 6 and Fig. 7. When the hydrogenation temperature is 923 K, lamellar δ hydrides can be observed in the alloy, as shown in Fig. 6a. The corresponding selected-area electron diffraction (SAED) patterns of δ hydride with $[011]_\delta$ zone axis suggest that the crystal structure of δ hydride is face-centered cubic (fcc). Fig.6b shows the precipitation of δ hydride in β phase. When hydrogen content exceeds the hydrogen saturation threshold in β phase, the reaction of β_H+H→δ occurs. Platelet α_2 phase can be observed in α matrix, as shown in Fig. 6c. The corresponding SAED patterns of α phase with $[\bar{1}101]_\alpha$ zone axis and α_2 phase with $[\bar{1}102]_{\alpha_2}$ zone axis suggest that the crystal structure of α_2 phase is hcp. When the hydrogenation

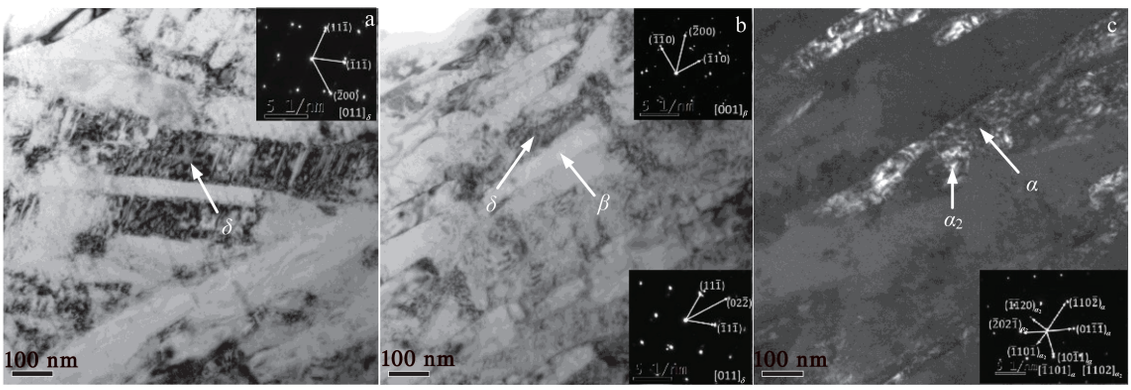

Fig.6 TEM images and SAED patterns of Ti6Al4V alloy hydrogenated at 923 K: (a) lamellar δ hydrides; (b) δ hydride precipitated in β phase; (c) dark field image of α_2 phase

temperature increases to 1023 K, the observed α' martensite and α'' martensite are parallel, as shown in Fig.7a, which also shows the corresponding SAED patterns of α' martensite with $[1\bar{2}1\bar{3}]_{\alpha'}$ zone axis and α'' martensite with $[001]_{\alpha''}$ zone axis. In addition, δ hydride twins can be observed in Ti6Al4V alloy hydrogenated at 1023 K, as shown in Fig.7b. The lamellar δ hydrides precipitated in Ti6Al4V alloy hydrogenated at 1023 K are thinner than those lamellar δ hydrides precipitated in Ti6Al4V alloy hydrogenated at 923 K (Fig.6a). The amount of δ hydride regions decreases when hydrogenation temperature increases from 923 K to 1023 K, indicating that δ hydrides become more unstable with increasing the hydrogenation temperature.

2.4 Discussion

According to the experiment results, it can be concluded that the Ti6Al4V alloys have different Sieverts constants and phase composition after hydrogenation at different temperatures. The hydrogen saturation in β phase (42.5at% H) is higher than that in α phase (4.7at% H), as shown in the phase diagram of Ti-H[21]. The mass percent of α phase in the as-received Ti6Al4V alloy is about 83.8wt%[22]. Therefore, most hydrogen dissolves in α phase during the hydrogenation treatment of Ti6Al4V alloy. When hydrogen content exceeds the hydrogen saturation threshold in α phase, the transformation of $\alpha_H \rightarrow \alpha_H+\beta_H$ occurs. With increasing the hydrogen content, the reaction of $\beta_H+H \rightarrow \delta$ occurs when hydrogen content exceeds the hydrogen saturation threshold in β phase. Therefore, the phase transformation of Ti6Al4V alloy during hydrogenation treatment can be expressed as follows: $\alpha+\beta \rightarrow \alpha_H+\beta_H \rightarrow \alpha_H+\beta_H+\delta \rightarrow \beta_H+\delta$. The phase transformations of $\alpha_H \rightarrow \alpha_H+\delta$ and $\beta_H \rightarrow \beta_H+\delta$ happen during the cooling process of the hydrogenated alloys[23]. The phase composition of Ti6Al4V alloys hydrogenated at 823 and 923 K is similar but different from the case at 1023 K. When the hydrogenation temperatures are 823 and 923 K, α_2 phase can be observed in the hydrogenated Ti6Al4V alloys. The formation of α_2 phase is attributed to the decrease of β transus temperature after hydrogenation and the enrichment of Al in α phase[20,23]. Based on the phase diagram of Ti-H[21], δ hydride cannot be precipitated in α phase at high temperature. However, when the hydrogenated Ti6Al4V alloy is cooled to room temperature, δ hydride can be precipitated in α_H phase due to the reduction of hydrogen solubility in α phase. In addition, the Sieverts constant is increased with increasing the hydrogenation temperature from 823 K to 923 K. When the hydrogenation temperature is 923 K, the amount of β phase

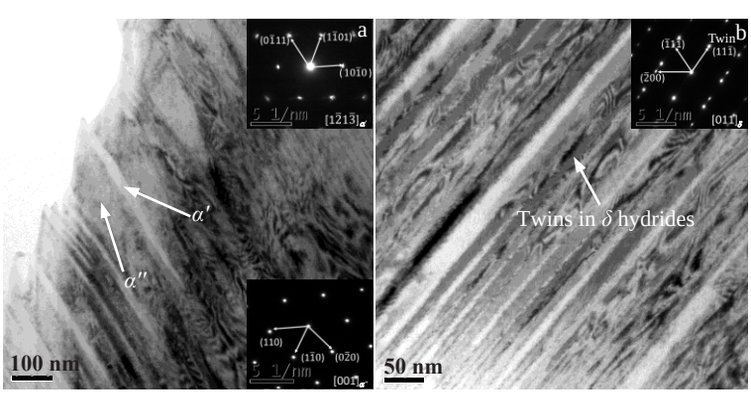

Fig.7 TEM images and SAED patterns of Ti6Al4V alloy hydrogenated at 1023 K: (a) α' and α'' martensite; (b) twins in δ hydrides

and δ hydride is larger than that of the Ti6Al4V alloy hydrogenated at 823 K, and a large amount of hydrogen dissolves in β phase and δ hydride. α_2 phase disappears when the hydrogenation temperature increases to 1023 K, because α_2 phase is completely transformed into α phase at higher temperatures[22]. Tiny acicular α' martensite and wide acicular α" martensite appear in Ti6Al4V alloy when the hydrogenation temperature is 1023 K. β phase is transformed into α' martensite and α" martensite during the cooling process of Ti6Al4V alloy hydrogenated 1023 K. Because part of β phase does not have enough β-stabilizing elements, the eutectoid reaction of $\beta\rightarrow\alpha$' occurs during the cooling process. Part of β phase is transformed into α" martensite due to the redistribution of β-stabilizing elements in the alloy during the hydrogenation treatment[24,25]. The Sieverts constant is decreased with increasing the hydrogenation temperature from 923 K to 1023 K. β phase becomes the main phase which dissolves plenty of hydrogen, but δ hydride becomes unstable and even decomposes. In general, the Sieverts constant is related to the amount of different phases and hydrogenation temperature.

3 Conclusions

1) Hydrogen pressure is increased with increasing the hydrogen content when Ti6Al4V alloy was hydrogenated at different temperatures. The pressure-composition (*P-C*) isotherms of Ti6Al4V alloy are divided into three regions. Only one pressure plateau exists during the hydrogenation treatment for each *P-C* isotherm of Ti6Al4V alloys hydrogenated at 823~973 K.

2) The values of enthalpy and entropy of the pressure plateau region are −50.7±0.26 kJ/mol and −138.4±0.69 $J\cdot K^{-1}\cdot mol^{-1}$, respectively.

3) The Sieverts constant increases firstly and then decreases gradually with increasing the hydrogenation temperature. The Sieverts constant reaches its maximum value when the hydrogenation temperature is 923 K.

4) The phase transformation of Ti6Al4V alloy during the hydrogenation treatment can be expressed as follows: $\alpha+\beta\rightarrow\alpha_H+\beta_H\rightarrow\alpha_H+\beta_H+\delta\rightarrow\beta_H+\delta$. The phase composition of Ti6Al4V alloys hydrogenated at 823 and 923 K is similar but different from that of Ti6Al4V alloy hydrogenated at 1023 K.

5) The Sieverts constant is related to the amount of different phases and hydrogenation temperature.

References

1 Yu Qiqi, Wen Daosheng, Wang Shouren *et al. Coatings*[J], 2020, 10(1): 52

2 Zhang Zhaohui, Liu Quanming, Liu Shifeng *et al. Rare Metal Materials and Engineering*[J], 2019, 48(1): 104

3 Yuan Baoguo, Liu Dahai, Li Chunfeng. *Rare Metal Materials and Engineering*[J], 2014, 43(9): 2104

4 Wang Xiaoli, Zhao Yongqing, Wei Xiaowei *et al. Transactions of Nonferrous Metals Society of China*[J], 2014, 24(1): 82

5 Li Miaosen, Zhang Weifu, Zhu Tangkui *et al. Rare Metal Materials and Engineering*[J], 2010, 39(1): 1

6 Yuan Baoguo, Du Jiangfei, Zhang Xiaoxue *et al. International Journal of Hydrogen Energy*[J], 2020, 45(46): 25 567

7 Ma T F, Chen R R, Zheng D S *et al. Materials Letters*[J], 2018, 213: 170

8 Yuan B G, Zheng Y B, Gong L Q *et al. Materials & Design*[J], 2016, 94: 330

9 Wang Xuan, Wang Liang, Luo Liangshun *et al. Journal of Alloys and Compounds*[J], 2017, 728: 709

10 Wen D S, Zong Y Y, Wang Y Q *et al. Materials Science and Engineering A*[J], 2016, 656: 151

11 Li Miaoquan, Zhang Weifu. *International Journal of Hydrogen Energy*[J], 2008, 33(11): 2714

12 Li Xifeng, Chen Nannan, Wu Huiping *et al. International Journal of Hydrogen Energy*[J], 2018, 43(27): 12 455

13 Grabovetskaya G P, Stepanova E N, Ratochka I V *et al. Materials Science Forum*[J], 2016, 838-839: 344

14 Zhang Xuemin, Cao Leilei, Zhao Yongqi *et al. Materials Science and Engineering A*[J], 2013, 560: 700

15 Shen C C, Perng T P. *Acta Materialia*[J], 2007, 55(3): 1053

16 Wang Xiaoli, Zhao Yongqing. *Rare Metals*[J], 2020, 39(12): 1413

17 Yuan Baoguo, Wang Yujie, Zheng Yubin *et al. Rare Metal Materials and Engineering*[J], 2017, 46(6): 1486

18 Nishikiori T, Nohira T, Ito Y. *Journal of the Electrochemical Society*[J], 2001, 148(1): E38

19 Zhu T K, Li M Q. *Materials Characterization*[J], 2011, 62(9): 852

20 Yuan Baoguo, Zheng Yubin, Wang Yujie *et al. Journal of Alloys and Compounds*[J], 2015, 648: 794

21 Zhu Tangkui, Li Miaoquan. *Journal of Alloys and Compounds* [J], 2009, 481(1-2): 480

22 Yuan Baoguo, Liu Xing, Du Jiangfei *et al. Journal of Materials Science & Technology*[J], 2021, 72: 132

23 Zhang Y, Zhang S Q. *International Journal of Hydrogen Energy* [J], 1997, 22(2-3): 161

24 Sun Zhonggang, Hou Hongliang, Zhou Wenlong *et al. Journal of Alloys and Compounds*[J], 2009, 476(1-2): 550

25 Qazi J I, Senkov O N, Rahim J *et al. Materials Science and Engineering A*[J], 2003, 359(1-2): 137

Ti6Al4V合金相变及吸氢热力学研究

张小雪[1]，杜江飞[2]，彭菲菲[3]，肖兴茂[3]，袁宝国[2]
(1. 安徽三联学院，安徽 合肥 230601)
(2. 合肥工业大学，安徽 合肥 230009)
(3. 西南技术工程研究所，重庆 400039)

摘　要：在823~1023 K的氢化温度范围内对Ti6Al4V合金进行了压力-成分等温线测试，研究了Ti6Al4V合金的相变和吸氢热力学。结果表明，当Ti6Al4V合金在不同的氢化温度下进行置氢处理时，氢压随着氢含量的增加而逐渐升高。由于Ti6Al4V合金中原始β相的存在，在置氢处理过程中，每个压力-成分等温线只有一个倾斜的压力平台。根据Vant's Hoff定律，压力平台区的焓变值和熵变值分别为-50.7±0.26 kJ/mol和-138.4±0.69 $J\cdot K^{-1}\cdot mol^{-1}$。随着置氢温度的升高，Sieverts常数呈先增大后逐渐减小的趋势。分析了Ti6Al4V合金在置氢处理过程中的相组成和相变。

关键词：钛合金；吸氢；热力学；相变

作者简介：张小雪，女，1985年生，硕士，讲师，安徽三联学院，安徽 合肥 230601，E-mail：540771788@qq.com